SCIENTIFIC REPORTS

OPEN

SUBJECT AREAS:
STRUCTURAL PROPERTIES
ASYMMETRIC SYNTHESIS

Received
30 September 2014

Accepted
17 December 2014

Published
20 January 2015

Correspondence and requests for materials should be addressed to S.E.S. (sarmiza.stanca@ipht-jena.de); C.K. (christoph.krafft@ipht-jena.de) or J.P. (juergen.popp@ipht-jena.de)

Aqueous Black Colloids of Reticular Nanostructured Gold

S. E. Stanca[1], W. Fritzsche[1], J. Dellith[1], F. Froehlich[1], A. Undisz[2], V. Deckert[1,3], C. Krafft[1] & J. Popp[1,3]

[1]Leibniz Institute of Photonic Technology, Albert-Einstein-Straße 9, 07745 Jena, Germany, [2]Otto Schott Institute of Materials Research, Friedrich Schiller University Jena, Löbdergraben 32, 07743 Jena, Germany, [3]Institute for Physical Chemistry and Abbe Center of Photonics, Friedrich Schiller University Jena, Helmholtzweg 4, 07743 Jena, Germany.

Since ancient times, noble gold has continuously contributed to several aspects of life from medicine to electronics. It perpetually reveals its new features. We report the finding of a unique form of gold, reticular nanostructured gold (RNG), as an aqueous black colloid, for which we present a one-step synthesis. The reticules consist of gold crystals that interconnect to form compact strands. RNG exhibits high conductivity and low reflection, and these features, coupled with the high specific surface area of the material, could prove valuable for applications in electronics and catalysis. Due to high absorption throughout the visible and infrared domain, RNG has the potential to be applied in the construction of sensitive solar cells or as a substrate for Raman spectroscopy.

In ancient Egypt, in the field known as *Chemi* at that time, the people utilised colloidal gold for its captivating optical effects. Over the years, this noble liquid has contributed to several aspects of life. It perpetually inspires people, leading to new and unpredictable applications. Currently, the size, shape, charge, and hydrophobicity of minuscule structures can be specifically engineered to create gold colloids with precise activity[1]. Three-dimensional plasmonic nano-arrays made of gold seem to be the future of electronic and optical multi-scaled devices[2–4]. In this challenging context, black gold[5,6] attracts scientific interest due to its optical properties, which suggest several potential applications[7,8]. Here, we report the finding of a unique form of gold, reticular nanostructured gold (RNG), as an aqueous colloid, with a broad absorption from the ultraviolet to the infrared, and present a method for its one-step synthesis. We also illustrate that the reticules consist of gold crystals that interconnect to form compact strands. How do the gold crystals evolve into a complex network? Which factors influence this anisotropic growth? Which way do the reticules assemble to absorb light from the ultraviolet to the infrared? Based on these questions and on our experimental evidence, a hypothetical structure of the reticule is proposed.

Generally, the anisotropic growth of nanocrystals in solution relies on the physico-chemical properties of the precursor and growth solutions[9]. Usually bimetallic crystals[10] or organic surfactants[11,12] promote the anisotropy of the system. The organic molecules selectively adhere to one face of the nanocrystal allowing its asymmetrical extension. To prepare red reticular gold, scientists utilise dendrimers[13], cyclodextrin[14] or aniline[15] as the organic initiator. In the present work, the network formation takes place by the simple addition of $NaBH_4$ to $HAuCl_4$ in the absence of organic molecules or other anisotropic external factors. This occurs at a very precise concentration ratio. The product is both black and reticular (§Methods). The low temperature, in conjunction with the concentrated growth solution, can generate localised anisotropy. The colloidal nanostructures (Fig. 1) (§Methods) remain stable for one week at room temperature. Subsequently, a black sediment appears, while the dark-grey supernatant is stable for many more months. With higher amounts of the reductive agent (§Methods), the colloid becomes unstable, although the colourless supernatant still contains reticular gold (Fig. 2a). The reticules seem to be shorter in the latter case. At lower concentrations of the reductive agent, the shapes become ellipsoidal (Fig. 2b) and spherical (Fig. 2c). These facts are consistent with our hypothesis that *upon adding an additional amount of* $NaBH_4$, a local anisotropy is created and the nanostructures switch from spherical (classical red colour) to reticular (black colour).

Results

RNG morphology. The RNG was investigated using electron microscopy and atomic force microscopy. The transmission electron and atomic force micrographs clearly illustrate a consistent reticular shape of the RNG (Fig. 1). A single strand has a length of 50 to 100 nm, a width of 10 ± 2 nm and a height of up to 3 nm. Similar

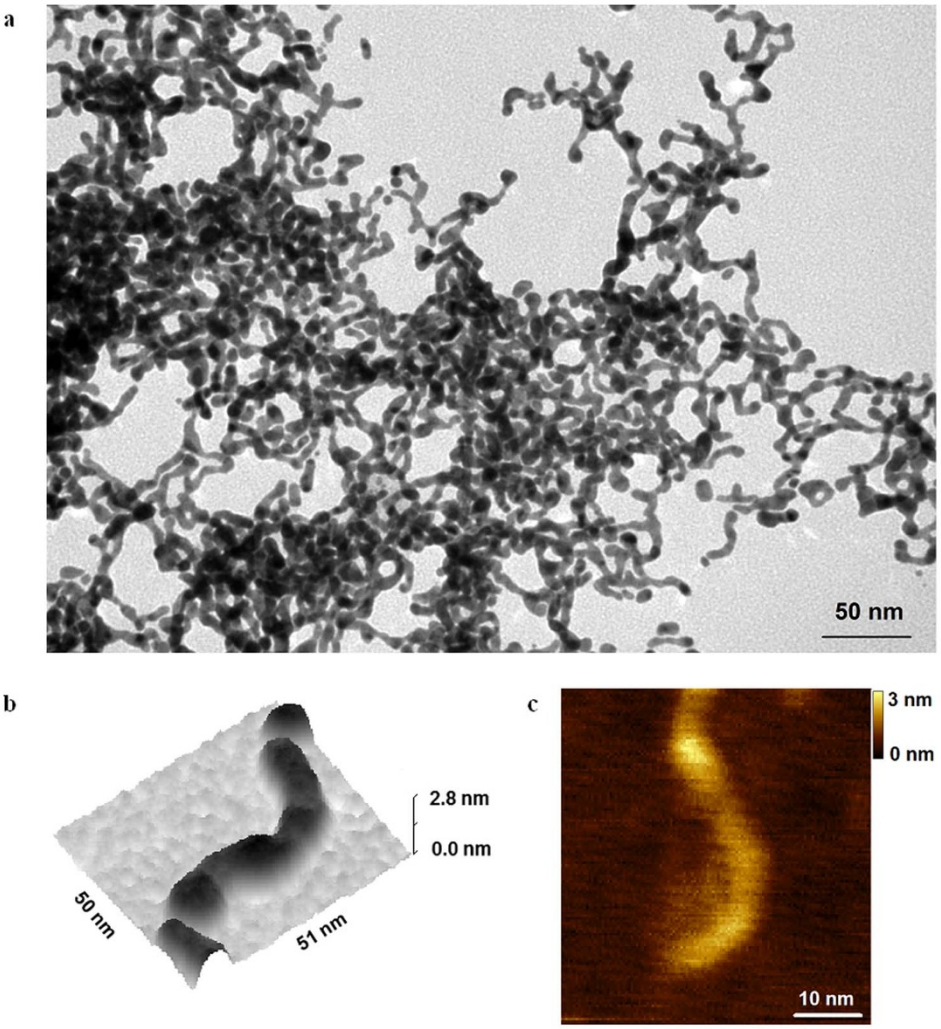

Figure 1 | **RNG morphology.** (a)–(b), TEM images of the RNG; (c), Atomic force micrograph of an individual reticule.

nanostructures were observed after several months of storing the solution at room temperature. SEM images of the nanostructures support the above findings, revealing a nanostructured conductive network (data not shown).

Light absorption characteristics. The RNG absorbance spectra in the ultraviolet-visible (UV-Vis) and infrared (IR) domains are presented in Figure 3. The colloidal dispersions of gold exhibit a broad absorption in the UV-Vis domain, as illustrated in Figure 3a. A plateau with two weak peaks in the green and near-infrared are observed. The weak peak at 530 nm is characteristic of the surface plasmon component of the colloidal gold. The band at longer wavelengths represents the longitudinal component, which can be associated with the presence of aggregates[7]. The absorbance naturally drops down in the case of supernatant however, the curve maintains a similar shape because it still contains reticules (Fig. 3a grey). How do these reticules couple to each other to absorb across the whole UV-Vis domain? To provide an answer to this question, we considered that different geometries permit the reticules to absorb a broad range of wavelengths. The reticular arrangement can only explain the extended absorption of light. The near-infrared spectrum of the RNG, spanning from 1000 to 2000 nm, overlaps well with the spectrum of water (data not shown). Fig. 3b compares the infrared spectra of RNG in water with pure water in the range 4000 to 500 cm^{-1} (corresponding to 2.5 to 20 μm wavelength). The bands of the main component water dominate the infrared spectra as expected. Diluted components can only generate weak bands. The most striking difference between the spectra of both samples is the offset for colloidal gold, which can be attributed to the colloid absorption. The second difference is a weak band at 2661 cm^{-1}, which can be assigned to BH_4^- [16,17], the precursor of the reducing mixture which was added in excess, compared to $HAuCl_4$. The part of BH_4^-, consumed for generation of H_2, was converted to $B(OH)_4^-$, however the infrared bands of this complex ion[18] are hidden by the prominent bands of water. Also, the second starting material $[AuCl_4]^-$ cannot be detected in the mid infrared range[19]. Consequently, BH_4^- is the single compound of the reaction mixture, detectable in the mid infrared range.

Structural characterisation of the RNG. X-ray diffraction (XRD) and energy dispersive X-ray spectrometry (EDX) were utilised to confirm the structure and composition of the RNG. Within the instrumental detection limits, the XRD pattern of the RNG identifies peaks for face-centred cubic (fcc) polycrystalline gold, with the small texture leading to an increase in the 111 reflex (Fig. 4a). By using the Scherrer formula and evaluating the spectrum shown in Fig. 4a, we estimated the crystallite size to be approximately 15 nm. This result is an average value over all spatial directions. Because of the high background in the spectra, the contribution of the smallest dimension (i.e., largest FWHM) may show a higher measurement error. Furthermore, there is no signal assigned to gold hydroxy complexes such as $Au(OH)_nCl_{4-n}$, which can be formed in a basic

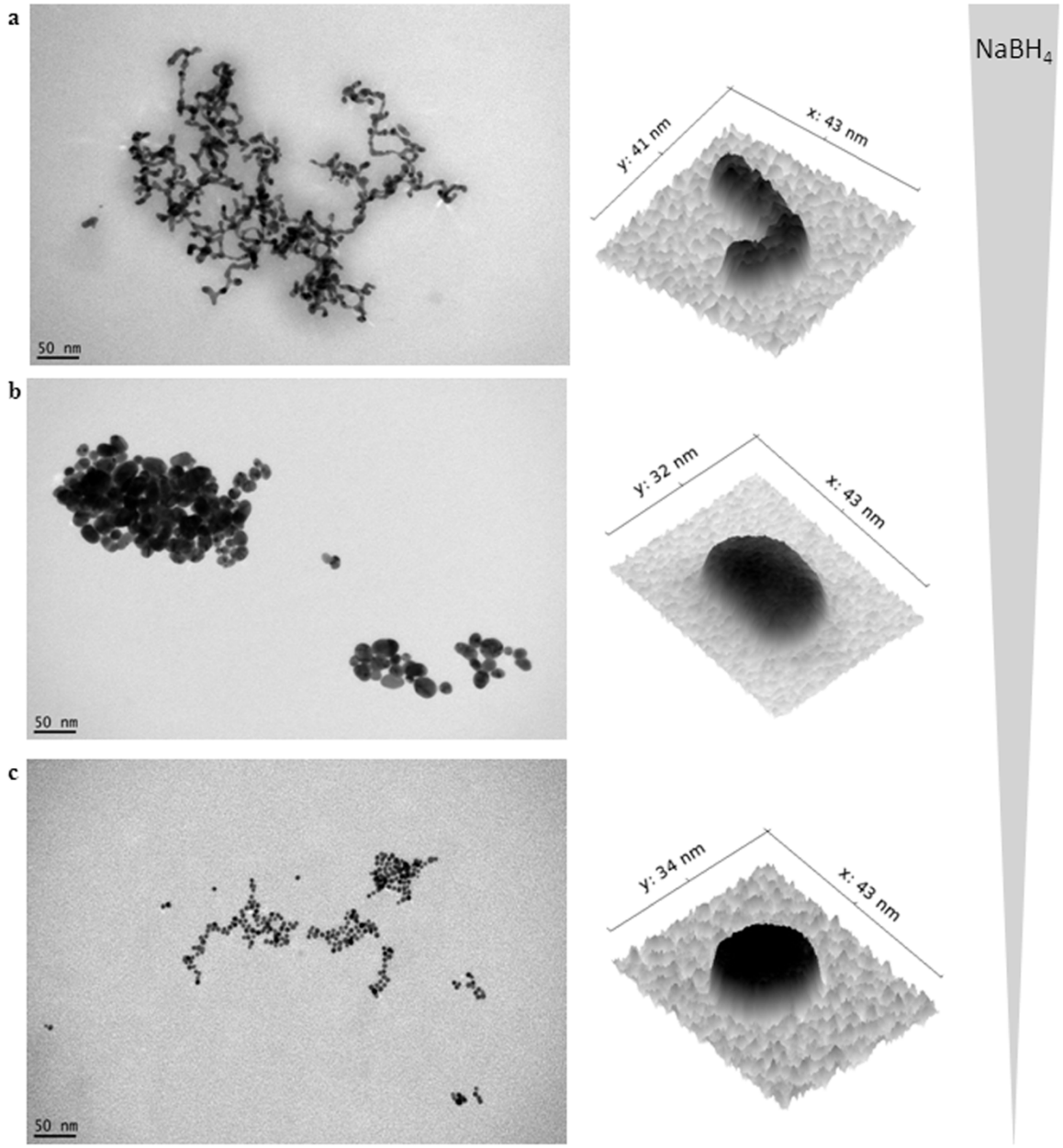

Figure 2 | The influence of the reductive agent concentration on the gold morphology. (a), TEM images of the nanostructure at higher amount of reductive agent; (b)–(c), TEM image of the nanostructures at lower amount of reductive agent (§ Methods).

dispersion[15]. For EDX measurements, micrometer-sized structures were deposited on amorphous carbon substrates. The spectra recorded at $E_0 = 5$ and 10 keV show high purity gold (Fig. 4b), with traces of sodium and chlorine. In the 5 keV spectrum, a weak Na-KL_3 (α) peak at nearly 1 keV is observable. The strong, unresolved peak at approximately 260 eV consists of both Au-$N_{4,5}N_{6,7}$ at 258 eV and C-KL_3 (α) at 277 eV, although the latter peak originates mainly from the carbon substrate used. In the 10 keV spectrum, a chlorine peak at 2620 eV appears, which 5 keV is insufficient to excite.

Discussion

The in-situ generated H_2 from the reaction

$$NaBH_4 + 4H_2O \rightarrow 4H_2 + NaB(OH)_4$$

stoichiometrically reduces the gold ions to isolated atoms via the reaction

$$HAuCl_4 + 1.5\ H_2 \rightarrow Au + 4HCl.$$

A further connection between the atoms creates nanostructures, with multiple assemblies possible. It is most likely that an excess of the tetrahedral anion BH_4^- initiates the anisotropy. These ions are preferentially adhered to the most instable face of the as-formed fcc Au crystal by the free electrons of boron. In addition, the water molecules, together with the mechanical convection generated by the gaseous hydrogen, play a key function in limiting the extension of the nanostructured chain. The growth of the reticule is controlled by adjusting the concentration of water and free hydrogen, thereby facilitating the slow selective addition of gold atoms to the most-unstable facet of the crystal[20], which in our case may be the {220}. The gold nanocrystals connect to each other by the {200} or {220} facets in an anisotropic path. The 311 faces are responsible for changing the angle of growth from 0° to 45° because of the {311} angle

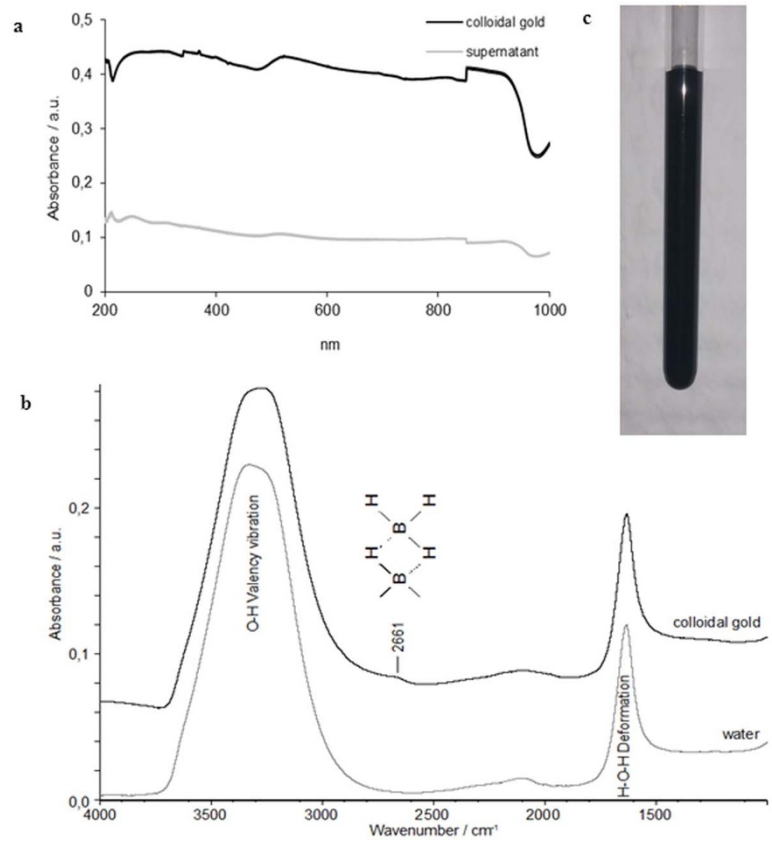

Figure 3 | Light absorption characteristics. (a), Absorbance spectra in UV-Vis of the 1 : 10 (v:v) diluted colloid; (b), IR spectrum of the colloidal gold compared with the spectrum of deionized water. Disturbing bands of the diamond crystal and of CO_2 were removed; (c), Photograph of the RNG colloid.

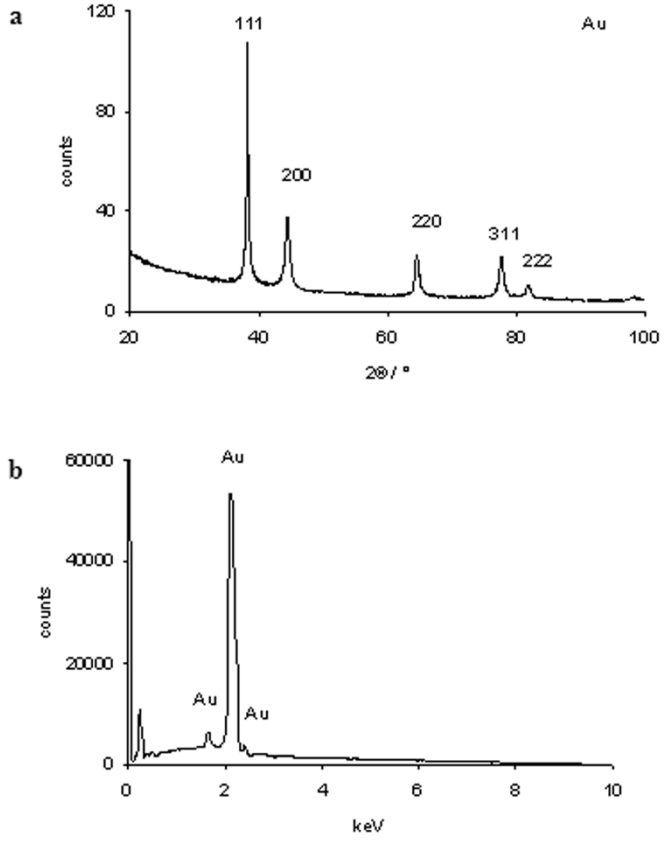

Figure 4 | RNG structure. (a), XRD pattern of the reticular black gold recorded using a Cu-K$\alpha_{1,2}$ radiation; (b), EDX pattern of the reticular black gold recorded at 10 keV radiation in 500 s.

plane, thus generating the curved structure. In this way, the fcc gold crystals form a nonlinear chain architecture surrounded by water and hydrogen molecules (Fig. 5a). The crystallinity was confirmed by high resolution TEM and Fast Fourier Transform image analysis (Fig. 5b).

This work demonstrated the existence of reticular gold nanostructures in aqueous black colloid after a one-step synthesis without any organic precursor. The reticules consist of a chain of gold crystals that interconnect to form compact strands a few nanometers high and wide and up to 100 nm long. This nanostructure gives an electrical conductivity of 4.47 ± 0.02 10^7 S/m, which is close to the reported value (4.52 10^7 S/m) for gold. Moreover, through exploiting its optical properties, RNG may find application in thermo-therapy, as an IR-absorbent, in Raman spectroscopy and in medical research. We anticipate that the newly introduced RNG will be rapidly adopted for widespread use in diverse fields of research and industry.

Methods

Colloidal gold preparation. All chemicals were purchased from Sigma-Aldrich (Taufkirchen, Germany, puriss p.a), except where otherwise mentioned. Colloidal gold preparation followed an adapted classical route[5]. The gold salt was reduced by hydrogen which was slowly released from $NaBH_4$ in aqueous solution. For synthesis two solutions were made; a gold salt solution containing 1 mL of 1% $HAuCl_4$ to 40 mL distilled water; and a reducing mixture consisting of 1 mL of 0.1% $NaBH_4$. At ice temperature the reducing solution was added to the gold salt solution under continuous stirring. The synthesis was completed when the black colour appeared (Fig. 3c). If instead the volume of the reductive agent increased to 2 mL the colloid becomes instable; sediment is formed and the colourless supernatant still contains reticular gold as shown TEM image (Fig. 2a). At lower amount of reductive solution (400 µL, 100 µL, respectively) the shapes become ellipsoidal (Fig. 2b) and spherical (Fig. 2c). The zeta potential of the colloids was consistently negative (−40 to −50 mV).

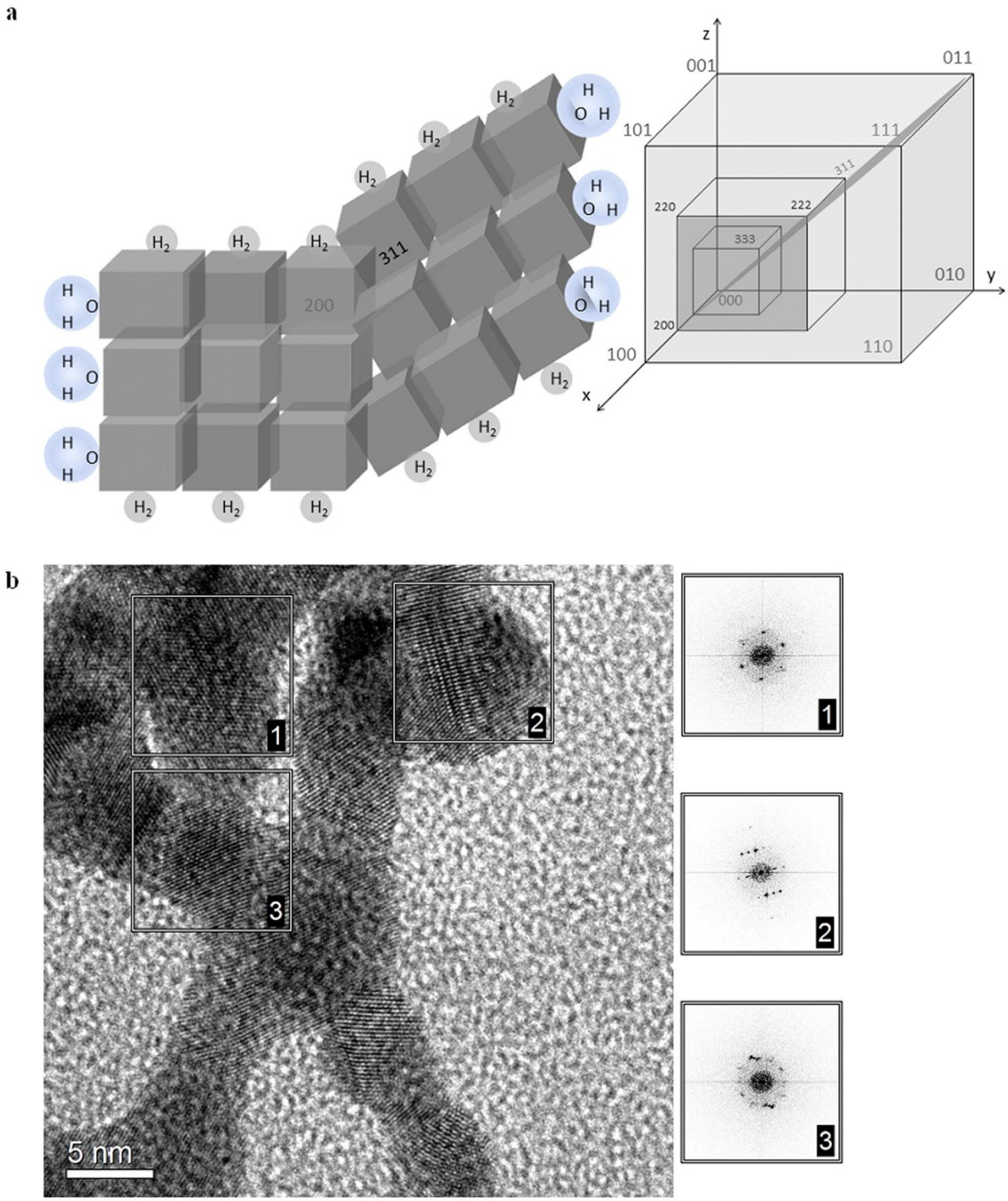

Figure 5 | Hypothetical assembly of the RNG. (a), The fcc Au crystals are articulate each other at the {200} or {220} facets. The {311} facet is responsible for changing the angle of growth. The hydrogen and water molecules limit the chain extension. (b), HRTEM of the reticules, the insets show the Fast Fourier Transform of the indicated areas.

Scanning Electron Microscopy (SEM). SEM measurements of the RNG were performed with a field emission microscope JSM-6300F (JEOL, Tokyo, Japan). The energy of the exciting electrons was mostly 5 keV. Beside the detector for secondary electrons (SEI) the system is equipped with different detector types (semiconductor and YAG type) for backscattered electrons. The sample preparation was done by the deposition of 10 μL droplets of the particle dispersion on polished amorphous carbon substrates (sigradur) and dried in air. Because of the low atomic number of carbon this strategy helps to increase the imaging contrast.

Atomic force microscopy (AFM). Atomic force micrographs were obtained using a MultimodeTM Nanoscope III (Digital Instrument s, Santa Barbara, CA, USA) instrument equipped with tapping mode silicon tips. Images were processed using Gwyddion open source software (http://gwyddion.net/).

Energy dispersive X-ray (EDX). EDX measurements were performed with a 30 mm^2 Si (Li) type detector from Oxford instruments (Abingdon, UK) and the INCA-Energy

evaluation software package. The specified energy resolution of the detector at 5.9 keV (Mn-Kα) amounts 133 eV.

Transmission Electron Microscopy (TEM). 5 μL of the particle dispersion, were deposited on a carbon coated 400 mesh copper grid. After 1 min of adsorption the excess liquid was blotted off with filter paper. Dried samples were then examined by a JEM 1400 (JEOL, Tokyo, Japan) transmission electron microscope. High Resolution Transmission Electron Microscopy (HRTEM) was performed using a TEM JEOL JEM-3010 operating at 300 keV.

X-Ray diffraction. The X-ray diffraction analysis has been performed with an X'pert Pro Instrument (PANanalytical, Almelo, Netherlands) using Cu-$K\alpha_{1,2}$ radiation. The Scherrer equation was used for the determination of the crystallite sizes. A droplet of colloid was dried on an amorphous substrate forming a loose bulk of random orientated gold nanostructures. Consequently, in the case of shape anisotropic structures all dimensions (length, width and height) contribute to the observed peak widths.

Spectrophotometry. UV-Vis spectra were obtained with a Jasco V-670 spectrometer (Hachioji, Tokyo, Japan) using plastic cuvettes (Brand GmBH Wertheim Germany).

Infrared Spectroscopy. The infrared spectra of the colloidal gold specimens were measured with the technique of Attenuated Total Reflectance (ATR) using a Single Reflectance Diamond ATR Cuvette in a FTIR-Spectrometer iS 10 (Thermo Fisher Scientific GmbH). The spectra were recorded with a resolution of 4 cm^{-1} in the spectral range 4000–500 cm^{-1}.

Size and zeta potential. The size and the zeta potential of the RNG colloid were recorded using a Zetasizer device (Malvern Instruments Ltd.). The dispersion was tested in a disposable sizing cuvette and a disposable zeta cell, respectively.

1. Weintraub, K. The new gold standard. *Nature* **495**, 14–16 (2013).
2. Hughes, M. D. *et al.* Tunable gold catalysts for selective hydrocarbon oxidation under mild conditions. *Nature* **437**, 1132–1135 (2005).
3. Boal, A. K. *et al.* Self-assembly of nanoparticles into structured spherical and network aggregates. *Nature* **404**, 746–748 (2000).
4. Crocker, J. C. Golden handshake. *Nature* **451**, 528–529 (2008).
5. Remy, H. [490] (Academic Press Geest & Portig, K.-G. Leipzig, 1961).
6. Pfund, A. H. The optical properties of metallic and crystalline powders. *J. Opt. Soc. Am.* **23**, 375–378 (1933).
7. O'Neill, P., Ignatiev, A. & Doland, C. The dependence of optical properties on the structural composition of solar absorbers: Goldblack. *Sol. Energy* **21**, 465–468 (1978).
8. Toyama, S., Takei, O., Tsuge, M., Usami, R., Horikoshi, K. & Kato, S. Surface plasmon resonance of electrochemically deposited Au-black. *Electrochem. Commun.* **4**, 540–544 (2002).
9. Liu, H., Zhang, X. & Gao, Z. Litography-free fabrication of large-area plasmonic nanostructures using colloidal gold nanoparticles. *Phot. Nano. Fund. Appl.* **8**, 131–139 (2010).
10. Habas, S. E., Hyunjoo, L., Radmilovic, V., Somorjai, G. A. & Yang, P. Shapping binary metal nanocrystals through epitaxial seeded growth. *Nature Mater.* **6**, 692–697 (2007).
11. Milliron, D. J., Hughest, S. M., Cui, Y., Manna, L., Li, J., Wang, L. W. & Alivisatos, A. P. Colloidal nanocrystal heterostructures with linear and branched topology. *Nature* **430**, 190–195 (2004).
12. Yin, Y. & Alivisatos, A. P. Colloidal nanocrystal synthesis and the organic-inorganic interface. *Nature* **437**, 664–670 (2005).
13. Gao, S., Zhang, H., Liu, X., Wang, X. & Ge, L. Room-temperatre strategy for networked nonspherical gold nanostructures from A(III)-[G-2]-CO_2H dendrimer complex. *J. Colloid. Interf. Sci.* **293**, 409–413 (2006).
14. Jia, H., Bai, X. & Zheng, L. Novel two-step synthesis of various gold nanostructures using Langmuir monolayer. *Colloid Surface A* **384**, 75–79 (2011).
15. Guo, Z. *et al.* One step controlled synthesis of anisotropic gold nanostructures with aniline as reductant in aqueous solution. *J. Colloid Interf. Sci.* **309**, 518–523 (2007).
16. Nakamoto, K. [473] (John Wiley& Sons Press, New York, 1986).
17. Günzler, H. & Böck, H. [250] (VCH Weinheim, 1983).
18. Davarajan, V., Gräfe, E. & Funck, E. Vibrational spectra of complex borates - II.$B(OH)_4^-$ - ion in teepleite, Raman spectrum and normal coordinate analysis. *Spectrochim. Acta* **30A**, 1235–1242 (1974).
19. Weidlein, J., Müller, U. & Dehnicke, K. [139] (Georg Thieme Press Stuttgart, New York, 1986).
20. Sun, Y. G. & Xia, Y. N. Shape-controlled synthesis of gold and silver nanoparticles. *Science* **298**, 2176–2179 (2002).

Acknowledgments

We thank Christa Schmidt for the XRD measurements and Franka Jahn for the TEM images. We are grateful to Prof. Dr. Rainer Heintzmann and Dr. Robert Müller for discussions.

Author contributions

J.D. performed the EDX, XRD measurements, FF recorded the FTIR spectra and AU accomplished the HRTEM and FFT. W.F., V.D., C.K. and J.P. provided materials, equipment and laboratory. All authors discussed and agreed the results. S.E.S. performed the synthesis designed the experiments and assembled the data together into a report. S.E.S., C.K. and J.P. wrote the paper.

Additional information

Competing financial interests: The authors declare no competing financial interests.

How to cite this article: Stanca, S.E. *et al.* Aqueous Black Colloids of Reticular Nanostructured Gold. *Sci. Rep.* **5**, 7899; DOI:10.1038/srep07899 (2015).